Conical sum-frequency generation in a bulk anomalous-like dispersion medium

Wanxu Zhao (赵婉旭)[1,2], Xiaohui Zhao (赵晓晖)[1,2], Yuanlin Zheng (郑远林)[1,2], Huaijin Ren (任怀瑾)[3], and Xianfeng Chen (陈险峰)[1,2,*]

[1]*State Key Laboratory of Advanced Optical Communication Systems and Networks, Department of Physics and Astronomy, Shanghai Jiao Tong University, Shanghai 200240, China*

[2]*Key Laboratory for Laser Plasmas (Ministry of Education), Collaborative Innovation Center of IFSA (CICIFSA), Shanghai Jiao Tong University, Shanghai 200240, China*

[3]*Institute of Applied Electronics, China Academy of Engineering Physics, Mianyang 621900, China*

**Corresponding author: xfchen@sjtu.edu.cn*

Received August 25, 2017; accepted October 27, 2017; posted online November 22, 2017

We observe conical sum-frequency generation in a bulk anomalous-like dispersion medium, which is attributed to complete phase-matching of one fundamental wave and the scattering wave of the other fundamental wave. In addition, efficient sum-frequency output is achieved making use of total internal reflection with conversion efficiency of 7.9% by only one reflection. The experiment proposes a new phase-matching mode under an anomalous-like dispersion condition, which suggests potential applications in efficient frequency conversion.

OCIS codes: 190.0190, 190.5890, 140.3613.
doi: 10.3788/COL201715.121901.

The process of efficient sum-frequency generation (SFG) has been studied a lot in previous researches. The conversion efficiency of the SFG process depends crucially on the phase-matching relationship between three interacting waves. One of the interacting beams could be substituted by the scattering light in some degenerated SFG processes, which may refer to the interaction of the incident light with a refractive-index inhomogeneity on the micro-scale in a bulk crystal[1]. This usually leads to many types of parametric scattering processes that behave as particular light patterns, such as points, lines, and rings[2,3]. As the theory of quasi-phase-matching (QPM) first proposed by Bloembergen *et al.* in 1962[4], it provides diverse types of phase-matching geometries in one-dimensional (1D) and two-dimensional (2D) $\chi^{(2)}$ nonlinear crystals. Recently, the generation of scattering second harmonic (SH) rings in a 1D quasi-periodical and a 2D periodical optical super-lattice has been presented[5–7]. Moreover, observation of scattering-assisted conical SFG in a 1D periodical photonic crystal has been reported[8]. In the above previous reports, an optical super-lattice is employed, and the reciprocal lattice vectors are involved for frequency conversion. But, for bulk material, scattering-assisted conical SH generation (SHG) or SFG is not observed because of phase-mismatching. Here, we structure the anomalous-like dispersion condition to generate conical SFG in a bulk medium. Using birefringent crystals, the refractive index of ordinary fundamental light can be greater than the extraordinary polarized sum-frequency (SF) under specific wavelengths, where we called it anomalous-like dispersion. Under this anomalous-like dispersion condition, the fundamental light and the SF could satisfy a complete triangle phase-matching relationship and generate efficient SF output.

Moreover, SFG is always used to transfer a relatively weak infrared incident signal into the visible range, taking advantage of strong visible light or a near-infrared pump laser. Using the SFG up-conversion process to detect infrared signals and infrared images has a lot of possibilities and advantages[9–12], which particularly shows its importance as the foundation of nonlinear infrared spectroscopy[13–15]. Previous experiments showed that the photon conversion efficiency can be close to 100%, which utilized an $LiIO_3$ crystal and a 0.6943 μm ruby laser pump to get the SFG for the 3.39 μm infrared signals[16]. SFG is also an effective means for producing new coherent radiation using dual-wavelength Nd:$YAIO_3$ lasers, and an $LiIO_3$ crystal to get SFG could directly access the 413.7 nm violet radiation[17].

In this Letter, we report on conical SFG in a bulk nonlinear medium with anomalous-like dispersion, which is derived from complete phase-matching of one fundamental wave and the scattering wave of the other fundamental wave. Based on this phase-matching scheme, we took advantage of total internal reflection to gain the single pass conversion efficiency of 7.9% by just one reflection.

To demonstrate the conical SFG, two collinear laser beams with frequencies ω_1 and ω_2 are mildly focused into a nonlinear crystal, as shown in the experimental setup in Fig. 1(a). The light source is an optical parametric amplifier (OPA, TOPAS, Coherent Inc.) pumped by a Ti:Sapphire femtosecond regenerative amplifier system (50 fs duration, 1 kHz repetition rate). Two wave beams from the OPA, the residual pump (F1) centered at 800 nm, and the signal (F2), tunable from 1000 to 1600 nm (both ordinarily polarized), are synchronized and loosely focused into the sample along the X axis. The waist diameter of the beams is about 50 μm and focused on the interior of the crystal. The mirror

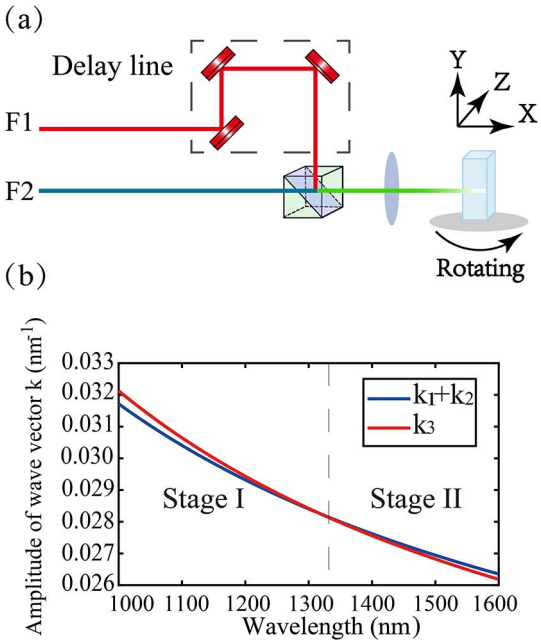

Fig. 1. (Color online) (a) Layout of experimental setup. $\lambda_1 = 800$ nm, $\lambda_2 = 1000$–1600 nm. (b) Theoretical curves of the wave vector relationship of the interaction beams, where the incidences are both set to ordinary polarized, and the SFG is extraordinary polarized.

arrangement is a delay line to synchronize these two pulses. This mirror arrangement is placed on a translation stage, which could continuously change the optical path of F1. When the pulses of these two beams overlapped spatio-temporally, we could achieve the most efficient nonlinear interaction. The sample used in the experiment is a z-cut 5 mol% MgO:$LiNbO_3$ crystal with dimensions of 3 mm×10 mm×2 mm ($X \times Y \times Z$).

The dispersion curve of SFG varying with incident wavelength under the oo-e phase-matching condition is shown in Fig. 1(b), where k_1, k_2, and k_3 are the wave vectors of the fundamental waves and harmonic wave, respectively. There are two stages of the wave vectors relationship among the interaction beams: Stage I $k_1 + k_2 < k_3$, Stage II $k_1 + k_2 > k_3$. Stage I shows the normal dispersion circumstance where the collinear SF and scattering SH ring of F2 could be expected, but there is no conical SFG. As for Stage II, corresponding to anomalously dispersive media, collinear SFG and two conical SFGs could be observed. In both Stages I and II, the scattering SH ring of F1 could not be observed.

In our experiment, patterns with the wavelength of F2 are tuned across the range of 1240–1320 nm for the first stage, where $k_1 + k_2 < k_3$ are demonstrated in Fig. 2(a). The scattering SH ring of F2 could be observed, whose generation is derived from complete phase-matching of the incident light F2 and the scattering light of F2. As Fig. 2(b) shows, $\vec{k}_1$ and $\vec{k}_2$ are the wave vectors of the ordinary polarized fundamental wave and extraordinary polarized SH, respectively. The arcs represent the birefringence effect. The radius of the red arc equals $|\vec{k}_2| + |\vec{k}_2'|$,

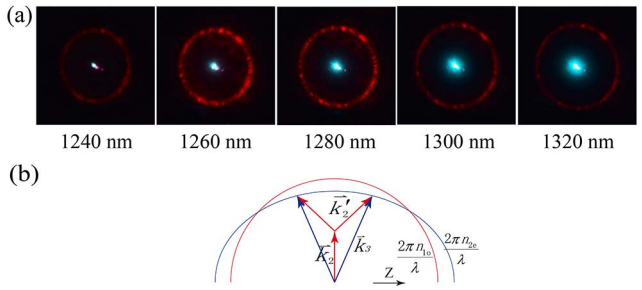

Fig. 2. (Color online) (a) Patterns on the screen by adjusting the wavelength of F2 from 1240 to 1320 nm. (b) The phase-matching diagram of the conical SH beam.

and the distance from the center to the blue arc equals $|\vec{k}_3|$ in different directions. The incident fundamental wave $\vec{k}_2'$ propagates along the X axis of the sample. Previous researchers have found that the scattering light can provide an additional fundamental wave $\vec{k}_2'$, in both bulk crystals[18,19] and in super-lattice crystals[5–7]. The scattering is ascribed to the interaction of the incident light with a refractive-index inhomogeneity on the micro-scale in the bulk crystal. Besides the imperfections on the surface and inside the crystal, impurity ions are the most important scattering sources[20,21]. Thus, the phase-matching relationship could be realized as

$$\vec{k}_3 - \vec{k}_2 - \vec{k}_2' = 0. \tag{1}$$

The scattering SH ring of F1 could not be observed because the wave vector of F1, scattering light, and SH could not satisfy Eq. (1). Moreover, the central spot is composed of the collinear SFG, and the collinear SH beams of F1 and F2. There is no conical SFG in the normal dispersion environment, which is in agreement with our theoretical prediction.

When the incident wavelengths reach Stage II, where $k_1 + k_2 > k_3$, Fig. 3(a) shows the experimental conical SFG patterns with the wavelength of F2, ranging from 1420 to 1560 nm; the phase-matching condition is illustrated in Fig. 3(b), where $\vec{k}_1$, $\vec{k}_2$, and $\vec{k}_3$ are the wave vectors of the ordinary polarized F1, F2, and the extraordinary polarized SF, respectively. The incident fundamental waves $\vec{k}_1$ and $\vec{k}_2$ propagate along the X axis of the sample.

In the experiment, $\vec{k}_1'$ and $\vec{k}_2'$ represent the scattering light of F1 and F2, respectively, which provide the additional fundamental waves. Thus, two conical SFGs could be observed on the screen. The inner SF ring is derived from complete phase-matching of F1 and the scattering light of F2, while the outer SF ring is derived from complete phase-matching of F2 and the scattering light of F1. Moreover, there also could be a scattering SH ring of F2 in theory, but it was not observed in the experiment because the intensity of F2 is low.

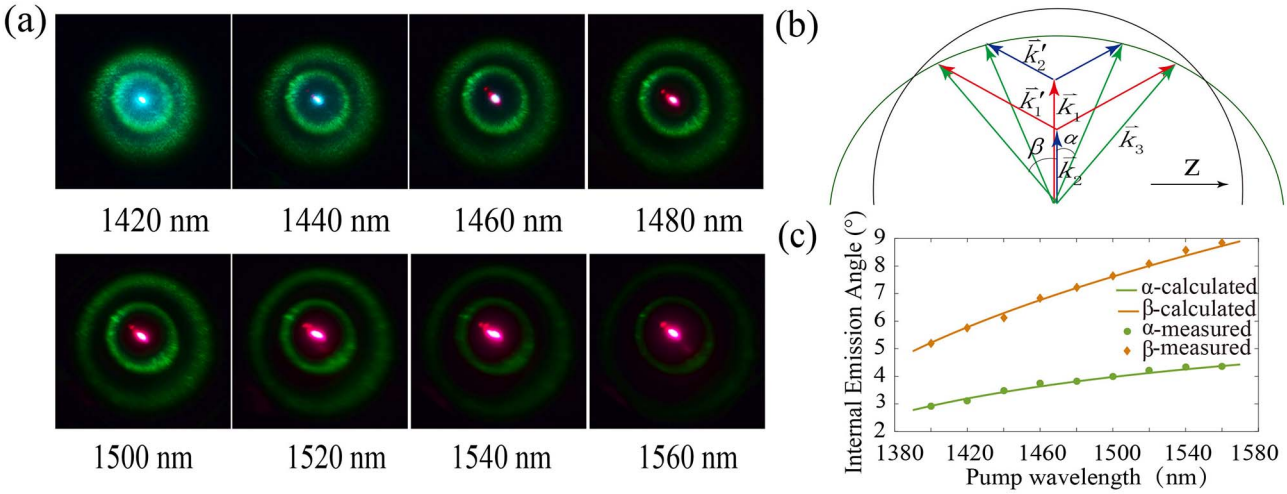

Fig. 3. (Color online) (a) Conical SFG patterns with the wavelength of incidence F2 from 1420 to 1560 nm. (b) Diagram of complete phase-matching condition of conical SFG. (c) The internal emission angles α and β as a function of the pump wavelength.

A triangle phase-matching relationship could be realized as

$$\vec{k}_3 - \vec{k}_1 - \vec{k}_2' = 0, \tag{2}$$

$$\vec{k}_3 - \vec{k}_2 - \vec{k}_1' = 0. \tag{3}$$

The internal emission angles α and β for the inner and outer rings are defined as the half apex angle of the conical SFG in the crystal. According to the cosine theorem, α and β satisfy

$$\cos\alpha = \frac{k_1^2 + k_3^2(\alpha) - k_2'^2}{2k_1k_3(\alpha)}, \tag{4}$$

$$\cos\beta = \frac{k_2^2 + k_3^2(\beta) - k_1'^2}{2k_2k_3(\beta)}. \tag{5}$$

The relationship between the pump wavelength and the internal emission angles α and β based on Eqs. (4) and (5) are shown in Fig. 3(c), which fits the measured values well.

The SF intensity can be expressed as $I_3 \propto I_1 I_2' L^2$, where L is the interaction length, and I_1 and I_2' are the intensity of incident light F1 and scattering light of F2, respectively. It indicates that the SF conversion efficiency is restricted by the intensity of scattering light. If replacing the scattering light with a stronger one, the conversion efficiency can increase greatly. Here, we make use of total internal reflection inside the crystal to provide another fundamental frequency component. Under this method, by adjusting the direction of incident light, one can produce high efficiency SF output.

In the experiment, the sample was placed on a rotation table in its X–Z plane, as shown in Fig. 1(a), so that the incident angle θ included by the incident light and the crystal's X axis could be adjusted. When the incident light met the internal surface, the two SF rings were split into four rings. The other two rings were derived from the reflected light and its scattering light. Due to the total internal reflection on the internal surface, a part of the conical SFG could not get out of the crystal, so the rings were always incomplete, as shown in Fig. 4(a). When increasing the incident angle until ring 1 and ring 4 were tangent, meanwhile, rings 2 and 3 were tangent, the SF intensity was significantly enhanced at the two points of tangency, as shown in the second photograph in Fig. 4(a). At this moment, both $\vec{k}_1$, $\vec{k}_2'$ and $\vec{k}_{2re}$, $\vec{k}_1''$ constitute a triangle phase-matching relation with the SF $\vec{k}_3$, as shown in Fig. 4(b), where $\vec{k}_{2re}$ represents the reflected light of $\vec{k}_2$, and $\vec{k}_1''$ is the scattering light of $\vec{k}_{1re}$; the reflected light $\vec{k}_{2re}$ and the scattering light $\vec{k}_2'$ were just parallel, so $\vec{k}_2'$ could be replaced by $\vec{k}_{2re}$, and the SFG efficiency would be increased greatly. As the same, $\vec{k}_1'$ could be replaced by $\vec{k}_{1re}$, where $\vec{k}_{1re}$ is the reflected light of $\vec{k}_1$, so two enhanced SF points could be observed. The propagation process of the beams in the crystal is shown in the Fig. 4(c) when incident light, reflected light, and SFG are completely phase-matched, where the main role of reflected light in frequency conversion is just depicted. This process still has the participation of scattered light; even scattered light contributes very little to frequency conversion. The dispersion is neglected in the figure, as its effect is very weak.

The full width at half-maximum (FWHM) of phase-matching SF is about 7 nm, although the bandwidth of F2 is about 75 nm; namely, the efficient conversion efficiency is narrowband, which is the same as the birefringence phase-matching (BPM). This is because an incident angle only corresponds to a certain phase-matching frequency. Considering the different refractive index of F1 and F2, the external incident angle θ satisfies

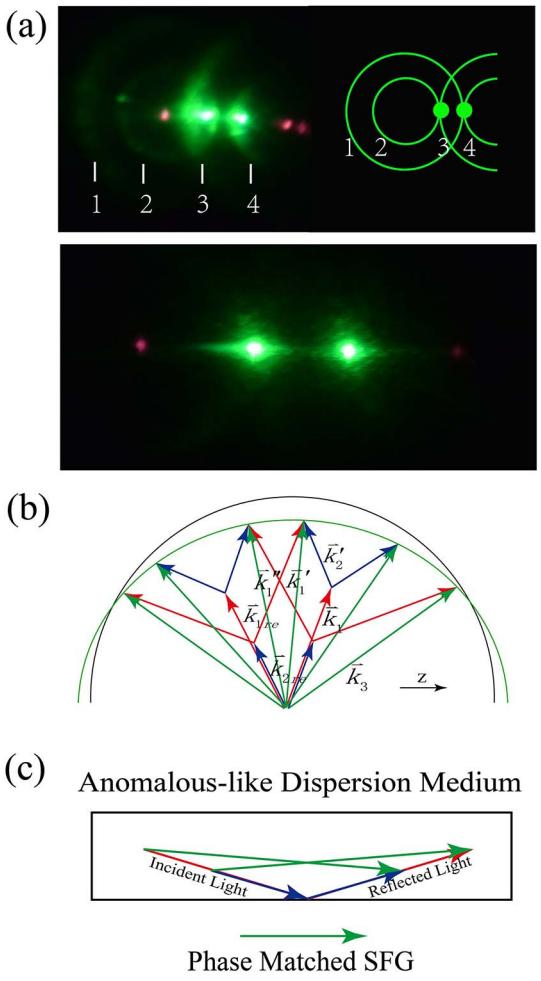

Fig. 4. (Color online) (a) Enhanced SFG patterns at the wavelength of incidence F2 of 1480 nm; the photograph below is the phase-matching SFG at two tangent points (see Visualization 1). (b) Diagram of phase-matching condition at the situation where the two SF rings are tangent. (c) Scheme of complete phase-matching by total reflection under the anomalous-like dispersion condition.

$$\pi - a\sin\left(\frac{\sin\theta}{n_{1o}}\right) - a\sin\left(\frac{\sin\theta}{n_{2o}}\right) = a\cos\left(\frac{k_1^2 + k_{2re}^2 - k_3^2}{2k_1 k_{2re}}\right). \quad (6)$$

Figure 5(a) shows the relationship of the center wavelength of F2 and external incident angle θ at the phase-matching condition according to Eq. (6), and the experimental data is consistent with the theoretical prediction.

The conversion efficiency is a key aspect that we concentrate on in this experiment. We measured the SFG output power at different wavelengths. Although each wavelength desires different phase-matching angles, their conversion efficiency makes little difference, as shown in Fig. 5(b). The power of F2 of different wavelengths from 1420 to 1480 nm decreased due to the OPA output characteristics; concomitantly, the SFG output power decreased. The SFG average power divided by

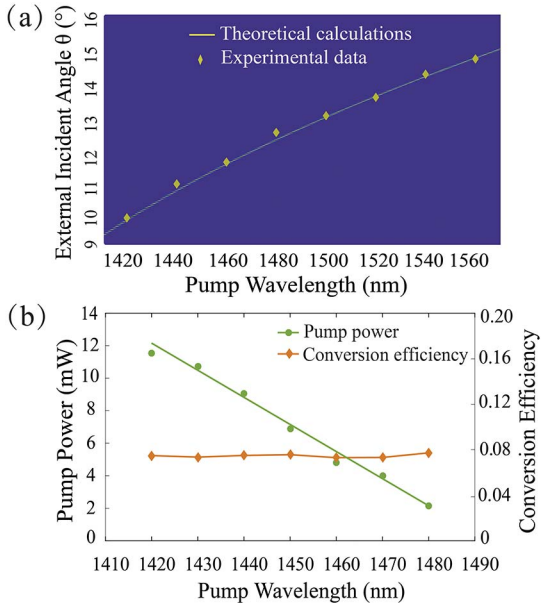

Fig. 5. (Color online) (a) External incident angle depending on the pump wavelength at the phase-matching condition. (b) Measured pump power from 1420 to 1480 nm; the red rhombuses are relative conversion efficiency calculated based on the power of the pump wave and the SFG.

the average power of F2 is defined as the conversion efficiency. The maximum conversion efficiency we obtained was 7.9% at 1480 nm, where the average input power of F2 is 2.14 mW, and the SFG average output power is 0.17 mW.

In conclusion, the specific completely phase-matching conical SFG is generated in a bulk anomalous-like dispersion medium. Moreover, we observe the efficient SFG, which makes use of reflected light to provide another fundamental frequency component instead of the scattering light. Experimentally, SFG conversion efficiency can achieve 7.9% through one total reflection. This kind of frequency conversion process has high conversion efficiency, which has potential for practical applications.

This work was supported in part by the National Natural Science Foundation of China (Nos. 61235009, 61505189, and 11604206) and the Presidential Foundation of the China Academy of Engineering Physics (No. 201501023).

References

1. H. Ren, X. Deng, Y. Zheng, N. An, and X. Chen, Appl. Phys. Lett. **103**, 021110 (2013).
2. N. An, Y. Zheng, H. Ren, X. Deng, and X. Chen, Appl. Phys. Lett. **102**, 201112 (2013).
3. W. Hasi, H. Zhao, D. Lin, W. He, and Z. Lü, Chin. Opt. Lett. **13**, 061901 (2015).
4. J. Armstrong, N. Bloembergen, J. Ducuing, and P. Pershan, Phys. Rev. **127**, 1918 (1962).
5. Z. Xie, G. Zhao, P. Xu, Z. Gao, and S. Zhu, J. Appl. Phys. **101**, 056104 (2007).

6. P. Xu, S. Ji, S. Zhu, X. Yu, J. Sun, H. Wang, J. He, Y. Zhu, and N. Ming, Phys. Rev. Lett. **93**, 133904 (2004).
7. H. Huang, C. P. Huang, C. Zhang, D. Zhu, X. H. Hong, J. Lu, J. Jiang, Q. J. Wang, and Y. Y. Zhu, Appl. Phys. Lett. **100**, 022905 (2012).
8. N. An, Y. Zheng, H. Ren, X. Zhao, X. Deng, and X. Chen, Photon. Res. **3**, 106 (2015).
9. H. Zeng, J. Wu, H. Xu, K. Wu, and E. Wu, Phys. Rev. Lett. **92**, 143903 (2004).
10. H. Zeng, J. Wu, H. Xu, K. Wu, and E. Wu, Phys. Rev. Lett. **96**, 83902 (2006).
11. G. Wu, W. Li, E. Wu, and H. Zeng, Opt. Express **18**, 1000 (2010).
12. R. Cao, B. Gai, J. Yang, T. Liu, J. Liu, S. Hu, J. Guo, Y. Tan, S. He, W. Liu, H. Cai, and X. Zhang, Chin. Opt. Lett. **13**, 121903 (2015).
13. J. Warner, *Quantum Electronics* (Academic, 1975).
14. M. M. Abbas, T. Kostiuk, and K. W. Ogilvie, Appl. Optics **15**, 961 (1976).
15. R. W. Boyd and C. H. Townes, Appl. Phys. Lett. **31**, 440 (1977).
16. T. R. Gurski, Appl. Phys. Lett. **23**, 273 (1973).
17. H. Y. Shen, W. X. Lin, R. R. Zeng, Y. P. Zhou, G. F. Yu, C. H. Huang, Z. D. Zeng, W. J. Zhang, R. F. Wu, and Q. J. Ye, Appl. Phys. **72**, 4472 (1992).
18. J. Giordmaine, Phys. Rev. Lett. **8**, 19 (1962).
19. Y. Chen, K. Su, T. Lu, and K. Huang, Phys. Rev. Lett. **96**, 033905 (2006).
20. K. Bastwöste, U. Sander, and M. Imlau, J. Phys.: Condens. Matter. **19**, 156225 (2007).
21. Y. Ja, J. Opt. **21**, 41 (1990).